

**POSSIBLE SUPERFLUID PHASE OF
PARAHYDROGEN ON NANOPATTERNED
SURFACES**

by

Saheed A. Idowu

A thesis submitted in partial fulfillment of the requirements for the degree of

Master of Science

Department of Physics

University of Alberta

© Saheed A. Idowu, 2015

Abstract

We study by computer simulations the low temperature properties of small parahydrogen clusters (free clusters) and the effect of confinement on the energetics and superfluid properties in two-dimensions (2D). Computed energetics for the free clusters are in quantitative agreement with that reported in the only previous study [M. C. Gordillo and D. M. Ceperley, Phys. Rev. B **65**, 174527 (2002)], but a generally strong superfluid response is obtained for clusters with more than ten molecules. All the free clusters, including the smallest one, feature a well-defined, clearly identifiable solidlike structure; with only one possible exception, those with fewer than $N = 25$ molecules are (almost) entirely superfluid at the lowest temperature considered (i.e., $T = 0.25$ K), and are thus referred to as nanoscale “supersolids”. The superfluid response in the low temperature limit of the confined clusters is found to remain commensurate in magnitude to that of the free clusters, for clusters fewer than twenty molecules, within a wide range of depth and size of the confining well. The flexibility of the superfluid response is traceable to the “supersolid” character of these clusters. We explore the possibility of establishing a bulk 2D superfluid “cluster crystal” phase of p -H₂, in which a global superfluid response would arise from tunnelling of molecules across adjacent unit cells. Computed energetics suggests that for a cluster of about ten molecules, such a phase may be thermodynamically stable against the formation of the equilibrium insulating crystal, for values of cluster crystal lattice constant possibly allowing tunnelling across adjacent unit cells.

Acknowledgements

First and foremost, I would like to express my sincere gratitude to my supervisor, Professor Massimo Boninsegni for his patience, motivation, enthusiasm, and immense knowledge. His guidance helped me in all the time of research and writing this thesis. I could not have imagined having a better supervisor and mentor for my M.Sc study.

My sincere thanks also go to Tokunbo Omiyinka and Kingsley Emelideme, for their support, encouragement and help throughout this work. They both made my transition to Edmonton very smooth. Not forgetting Junaid Muhammad, Pavlovskii Konstantin, Elshamouty Khaled and Jose Avendano, I really appreciate you guys for your help.

I would also like to thank all my friends including Kunle Adeyanju, Ebele Ezeokafor, Micah Yusuf, Suleyman Yacoub, Adama Yatase, Haruna Ibrahim, Sulayman Oladepo and Olusanya Badejo, for their support in one way or the other.

My appreciation also goes to my parents for their prayers and encouragements. Also to my lovely wife, Olawunmi Sekinat, for her support, prayers and understanding. I cannot thank you enough.

Finally, the support from the Natural Science and Engineering Research Council of Canada (NSERC) grant and Westgrid are gratefully appreciated.

Table of Contents

1	INTRODUCTION	1
2	PHYSICAL MODEL AND METHODOLOGY	7
2.A	Many-body Hamiltonian	7
2.B	The Continuous-space Worm Algorithm	8
2.B.1	Thermal Averages and Path Integral Monte Carlo	9
2.B.2	Quantum Statistics	11
2.B.3	Conventional PIMC Permutation Sampling	12
2.B.4	Permutation Sampling In Worm Algorithm	12
2.B.5	Thermodynamic Estimators and Statistical Errors Evaluation	13
3	SYSTEMATICS OF SMALL PARA-HYDROGEN CLUSTERS IN TWO DIMENSIONS	16
3.A	Introduction	16
3.B	Model And Methodology	20
3.C	Results	21
3.D	Discussion	30
4	SUPERFLUID RESPONSE OF 2D PARAHYDROGEN CLUS-	

TERS IN CONFINEMENT	34
4.A Introduction	34
4.B Results	35
4.B.1 Superfluidity	35
4.B.2 Energetics	40
CONCLUSIONS	44
Bibliography	46

List of Figures

2.1	Permutation sampling in conventional PIMC	11
3.1	Energy per hydrogen molecule e (in K) versus cluster size N , at $T = 0.25$ K (full symbols). Also shown are the results reported in Ref. [15], at $T = 0.33$ K (open symbols). For clusters of size $N = 10, 13, 16$ and 20 , our energy estimates are indistinguishable from those of Ref. [15]. Statistical errors are at the most equal to symbol size.	22
3.2	(color online) Radial density profile for a cluster with $N = 7$ p -H ₂ molecules at $T = 0.33$ K (solid line). Filled circles show the corresponding result from Ref. [15]. Profiles are computed with respect to the center of mass of the cluster. Statistical errors are not visible on the scale of the figure. The local superfluid density profile for this cluster is indistinguishable from that of the local density.	23
3.3	(color online) Configurational snapshot (particle world lines) yielded by a simulation of a cluster with $N = 7$ p -H ₂ molecules at $T = 0.33$ K. Brighter colors correspond to a higher local density.	24

3.4	(color online) Radial density profile for cluster with $N = 13$ at $T = 0.33$ K (solid line). Also shown is the corresponding result from Ref. [15] (filled circles). Profiles are computed with respect to the center of mass of the cluster. Statistical errors are not visible on the scale of the figure.	26
3.5	(color online) Radial density profile for cluster with $N = 20$ at $T = 0.33$ K (solid line). Also shown is the corresponding result from Ref. [15] (filled circles). Profiles are computed with respect to the center of mass of the cluster. Statistical errors are not visible on the scale of the figure.	27
3.6	(color online) Radial density profiles for clusters with $N = 25$ (dashed line) and 26 (solid line) p -H ₂ molecules at $T = 0.25$ K. Profiles are computed with respect to the center of mass of the cluster. Statistical errors are not visible on the scale of the figure.	29
3.7	(color online) Configurational snapshot (particle world lines) yielded by a simulation of a cluster with $N = 25$ p -H ₂ molecules at $T = 0.25$ K. Brighter colors correspond to a higher local density.	30
3.8	(color online) Configurational snapshot (particle world lines) yielded by a simulation of a cluster with $N = 26$ p -H ₂ molecules at $T = 0.25$ K. Brighter colors correspond to a higher local density.	31
4.1	Superfluid fraction of 2D p -H ₂ clusters confined in a Gaussian well of size $\sigma = 3$ Å and depth $A = 40$ K (circles), $A = 60$ K (diamonds) and $A = 100$ K (triangles), at a temperature $T = 0.25$ K. Open triangles show results for free clusters. When not shown, statistical errors are at the most equal to symbol size. .	35

4.2	Configurational snapshots (particle world lines) yielded by a simulation of a cluster with $N = 20$ p -H ₂ molecules at $T = 0.25$ K. <i>Left</i> : Free cluster. <i>Right</i> : Cluster confined inside a gaussian well of depth $A = 100$ K and size $\sigma = 3$ Å. Brighter colors correspond to a higher local density.	36
4.3	Radial density profile for a cluster of $N = 20$ p -H ₂ molecules, confined in a Gaussian well of size $\sigma = 3$ Å and of depth $A = 100$ K. Dotted line shows the corresponding profile for a free clusters. These profiles are computed at $T = 0.25$ K. Statistical errors are not visible on the scale of the figure.	37
4.4	Superfluid fraction of 2D p -H ₂ clusters confined in a Gaussian well of size $\sigma = 6$ Å and depth $A = 20$ K (circles), $A = 60$ K (diamonds) and $A = 100$ K (triangles), at a temperature $T = 0.25$ K. Open triangles show results for free clusters. When not shown, statistical errors are at the most equal to symbol size. .	39
4.5	Energy per p -H ₂ molecule for clusters of N molecules ($1 \leq N \leq 30$), trapped in a well of size $\sigma = 3$ Å and depth $A = 60$ K (diamonds) and $A = 100$ K (triangles). Circles show the corresponding values for free clusters (i.e., $A = 0$). Statistical errors are smaller than symbol size. Horizontal line refers to the ground state energy per molecule of bulk p -H ₂ in its 2D crystal equilibrium phase.	40

Chapter 1

INTRODUCTION

The discoveries and inventions in the area of low temperature physics began in 1908 by Heike Kamerlingh Onnes, where he first liquified ^4He . He made precise measurements of liquid helium density and found that as the temperature is lowered, the density goes through a sharp maximum peak at ~ 2.2 K. This temperature was concluded by Willem Keesom and Mieczyslaw Wolfke in 1927 as the phase transition temperature (T_λ), they named the phase below T_λ as helium-II and the one above as helium-I [6].

A remarkable result was later discovered in 1937 by Kaptisa [1] and independently by Allen and Misener [2] that liquid helium-4 is superfluid. They both reported that liquid helium flowed with almost no measurable viscosity below the transition temperature of 2.18 K. The bizarre property such as zero viscosity was later attributed to the work of Lev Landau, Fritz London and Laszlo Tisza as an evidence of a new superfluid phase of matter. Superfluidity being associated with the motion of Bose-Einstein condensate (BEC) [3, 4] is still unclear even in a recent study [5]. Bose-Einstein condensation occurs when indistinguishable particles (Bosons) all occupy the same quantum me-

chanical state, this explains the reason why ^3He (another isotope of helium) cannot undergo BEC alone by themselves which is as a result of ^3He being fermion and also obeying Fermi statistics. A superfluid phase can only be observed by pairing up with fermions to form composite spin zero bosons which is observed at ≈ 2 mK. Such pairing mechanism results to superfluidity in superconductors [11] and in *all* Fermi systems.

Experimental investigation using oscillating disks reported by Keesom and Macwood shows that liquid helium is capable of being viscous and non-viscous at the same time [7]. This led to the formulation of two fluid model by Tisza and Landau [4, 8]. They independently postulated that at temperature below T_λ , helium-4 is made up of two fluids, namely the normal fluid (consisting of non-condensed atoms) and superfluid (non-viscous). At absolute zero temperature, it consists of superfluid only. The main difference between Tisza's theory and Landau's is in the nature of the normal component: it is made up of "quasiparticles" according to Landau.

Superfluids have been one of the most important discoveries in the 20th century, it allows us to see quantum mechanical behavior macroscopically. They possess interesting properties, such as amazingly high thermal conductivity [9] and the ability to flow without friction through narrow channels, for example superfluid film flow [10].

The search for superfluid phase in other elements aside helium has been an area of interest for a long time now. It has been predicted that spin-polarized atomic deuterium and tritium are fermionic and bosonic liquids respectively, in the zero temperature limit [12, 13]. However, their experimental study proves elusive as a result of their high recombination rate. The next candidate for superfluidity is molecular hydrogen, which is also known as parahydrogen ($p\text{-H}_2$).

The observation of its putative superfluid phase [36] has so far been prevented by its strong tendency to crystallize at low temperature. There exists, however, experimental [42] evidence that finite clusters of p -H₂ remain liquidlike down to temperatures much lower than the bulk crystallization temperature, conceivably allowing one to probe their predicted superfluid behaviour, expected to manifest itself at a temperature $T \sim 1$ K, for clusters of thirty molecules or less [43, 44, 45]. The question thus arises of whether one might be able to observe a *macroscopic* superfluid response in a network of interconnected superfluid clusters, in which global phase coherence could be established by tunnelling of molecules across adjacent clusters. This is, in a sense, analogous to the physics of the recently proposed supersolid phase of soft core bosons in 2D [14, 18, 19].

The above scenario could be achieved experimentally, for example, by adsorbing p -H₂ inside a porous material such as vycor [16, 17]. Another plausible avenue, perhaps affording greater control, exploits the predicted superfluid response of p -H₂ clusters confined to quasi 2D [15, 20]. The idea is that of fashioning a planar substrate capable of adsorbing p -H₂ molecules at specific sites, arranged on a regular triangular lattice, each designed to accommodate a number of molecules corresponding to a strong superfluid response at low temperature (i.e., around twenty [20]). The distance between nearest-neighboring clusters should be chosen to render such a cluster crystal energetically favorable with respect to the formation of the ordinary uniform, non-superfluid crystalline phase (with just one molecule per unit cell), while concurrently allowing tunnelling of molecules across nearest neighboring wells, each one acting in a sense like a superfluid quantum dot. Whether all of these conditions can be met is not *a priori* obvious, and furnishing a quantitative answer

is the goal of this work.

Aside from the energetics, a second aspect to assess quantitatively is the effect of confinement on the superfluid properties of the individual clusters, which, besides being obviously crucial to the goal of stabilizing the bulk superfluid phase described above, is of interest in its own right and might be probed experimentally, for example by trapping small clusters at adsorption sites of corrugated substrates [21]. On the one hand, spatial confinement is expected to bring about a reduction of the superfluid response of a structureless, liquidlike droplet, owing to the ensuing increased particle localization. However, in our first study [20] we established that 2D parahydrogen clusters of less than thirty molecules, turning superfluid at a temperature of the order of 1 K, display a rather marked “supersolid” character (obviously such a definition is necessarily loose, given that we are talking about a finite system); that is, although exchanges of identical molecules are frequent at low temperature, concurrently molecules are nonetheless spatially localized and form orderly structures. Thus, owing to their greater rigidity, superfluidity in these finite clusters may be robust against external confinement – more so than in helium droplets, for instance. Furthermore, it has been recently shown that confinement can actually have an *enhancing* effect on the superfluid response of *p*-H₂ clusters in three dimensions [22].

In order to investigate quantitatively the effect of confinement on its structure, energetics and superfluid properties, we have carried out first principle Quantum Monte Carlo simulations of a single, spatially confined 2D *p*-H₂ cluster at low temperature ($T = 0.25$ K). We studied clusters comprising up to thirty molecules. Confinement in this study is described by means of a simple gaussian well of varying size (typically of the order of a few Å) and depth (up

to 100 K).

We compared the computed superfluid response of the confined clusters with that of its free counterpart, it shows that while as expected superfluidity is suppressed in sufficiently deep wells, nonetheless clusters retain their structure and superfluid response within a rather wide range of confinement parameters, i.e., they are relatively unaffected by the confinement. Suppression of superfluidity takes place gradually as the well is deepened, affecting primarily the largest clusters. On the other hand, clusters with ~ 15 molecules or less remain superfluid, at the low temperature considered here, even when confined in fairly deep wells. Our physical conclusion is that, even making allowance for the simplicity of the model utilized, superfluid appears to be remarkably resilient in these intriguing few-body systems; phrased alternatively, the quantitative requirements on the strength and size of the confining well may not be particularly stringent, at least in terms of ensuring a significant, possibly observable superfluid response of confined clusters.

The energetics of the system, however, is such that, no matter what values of depth and size of the attractive well one chooses, the distance between adjacent wells must be taken rather large (close to twice the size of an individual cluster), in order for the low-density cluster crystal to be energetically stable against the formation of the equilibrium 2D crystal. Consequently, in such a cluster crystal tunnelling of molecules across adjacent sites, necessary to establish a global superfluid response, will be essentially absent, for practical purposes. Thus, much like others previously explored [40, 41], this approach to stabilize a bulk superfluid phase of p -H₂ appears unlikely to succeed.

The structure of this thesis is summarized as follows: in chapter 2, we describe the microscopic model of our calculation and also the computational

methodology utilized. We devote chapter 3 to analysing the results of our first study, describing the low temperature properties of 2D p -H₂ clusters comprising between $N = 7$ and $N = 30$ molecules. This led us to studying the effect of confinement on this small p -H₂ clusters and possible stabilization of its bulk superfluid phase, we discussed this in chapter 4. Finally, we outlined the main physical conclusion of our study and provide possible avenues to obtaining a bulk superfluid phase.

Chapter 2

PHYSICAL MODEL AND METHODOLOGY

This chapter focuses on the discussion of the physical model and methodology adopted for our study.

2.A Many-body Hamiltonian

Our system of interest is modeled as a collection of N parahydrogen (p -H₂) molecules, regarded as point particles of spin zero, moving in 2D in the presence of a confining potential. The quantum mechanical many-body Hamiltonian is given by

$$\hat{H} = -\frac{\hbar^2}{2m} \sum_{i=1}^N \nabla_i^2 + \sum_{i<j} v(r_{ij}) + \sum_i V(\mathbf{r}_i), \quad (2.1)$$

where $\hbar^2/2m = 12.031 \text{ K}\text{\AA}^2$, \mathbf{r}_i is the position of the i th p -H₂ molecule, $r_{ij} \equiv |\mathbf{r}_i - \mathbf{r}_j|$, v is the potential describing the interaction of a pair of molecules,

while V is the confining potential. We model V by means of a simple Gaussian well, centered at the origin, namely

$$V(r) = -A \exp\left(-\frac{r^2}{2\sigma^2}\right). \quad (2.2)$$

While a direct experimental realization of such a confining potential may not be straightforward (not to our knowledge anyway), it contains nonetheless all the relevant ingredients to afford qualitative insight into the physics of the system, with a small number of parameters, thereby rendering the interpretation of the results easier. We use the well-known Silvera-Goldman potential [49, 50] to describe the pair-wise interaction among p -H₂ molecules.

The thermodynamics and the structural properties of the above system at low temperature ($T = 0.25$ K) have been studied by means of Quantum Monte Carlo simulations based on the continuous-space Worm Algorithm [25, 26]. Details of the calculation are standards, analogous to those employed, for instance, in the simulation of trapped dipolar Bose systems [23, 24]. Besides the energy per molecule, we compute radial density profiles with respect to the centre of the well, as well as global and local superfluid response of the clusters, using standard estimators for finite systems [48, 55, 56].

2.B The Continuous-space Worm Algorithm

Path Integral Monte Carlo (PIMC) method is of great importance in the theoretical investigation of quantum many-body systems. Besides the quantitative results yielded for a wide range of physical systems, it also enables us to understand phenomena such as superfluidity and Bose-Einstein condensa-

tion at the microscopic level. Path Integral Monte Carlo (PIMC) is the only known method capable of furnishing an exact numerical estimates of physical observables for bose particles at finite temperature. In addition, regardless of the sign problem that is often encountered while dealing with Fermi systems, PIMC still provides approximate estimates comparable to other leading methods [27, 28]. We thus regard PIMC as a realistic method to investigate our calculation of interest based on the continuous-space Worm Algorithm.

2.B.1 Thermal Averages and Path Integral Monte Carlo

We wish to compute the thermal average of a physical observable $\hat{\mathcal{A}}$, for a many-body system with N indistinguishable particles in thermal equilibrium at temperature T , described by Eq. (2.1). This quantity is given by

$$\langle \hat{\mathcal{A}} \rangle = \frac{1}{Z} \text{Tr} (\hat{\mathcal{A}} \hat{\rho}) = \frac{1}{Z} \int dR \mathcal{A}(R) \rho(R, R, \beta) \quad (2.3)$$

where $R \equiv \mathbf{r}_1 \mathbf{r}_2 \dots \mathbf{r}_N$ is a collective coordinate referring to all N particles in the system; $\beta = 1/(k_B T)$ and K_B is the Boltzmann constant (set to 1 for simplicity); Z is the canonical partition function, which is of the form

$$Z = \text{Tr} \hat{\rho} = \int dR \rho(R, R, \beta), \quad (2.4)$$

$\rho(R, R, \beta)$ is the many-body density matrix given by

$$\rho(R, R, \beta) = \langle R | e^{-\beta \hat{H}} | R \rangle \quad (2.5)$$

with \hat{H} given by Eq. (2.1). The many-body density matrix is in most cases unknown for a system of interacting particles, using path integral formalism

proposed by R. P. Feynman [29] an expression for ρ could be obtained. We start by using the identity

$$e^{-\beta\hat{H}} \equiv (e^{-\tau\hat{H}})^P, \quad (2.6)$$

where $\beta = P\tau$, P is an identity operator, and τ is an imaginary time. Eq. (2.5) can then be written as

$$\begin{aligned} \rho(R, R, \tau) &= \langle R | e^{-\tau\hat{H}} e^{-\tau\hat{H}} \dots e^{-\tau\hat{H}} | R \rangle \\ &= \int dR_1 dR_2 \dots dR_{P-1} \prod_i \rho_o(R_i, R_{i+1}, \tau). \end{aligned} \quad (2.7)$$

For a fixed β , the many-body density matrix approaches the free-particle density matrix in the limit of large P (or small τ), in this limit, we obtain, to 3rd order in τ

$$\rho(R, R', \tau) \approx \rho_o(R, R', \tau) e^{-\tau V(R)}, \quad (2.8)$$

where $V(R) = \sum_{i<j} v(r_{ij}) + \sum_i V(\mathbf{r}_i)$ as given in Eq. (2.1) and $\rho_o(R, R', \tau)$ in D -dimensional configuration space is given by

$$\rho_o(R, R', \tau) = \rho_o(\mathbf{r}, \mathbf{r}', \tau) = \left(2\pi\hbar^2\tau/m\right)^{-D/2} \exp\left[-\frac{m(\mathbf{r} - \mathbf{r}')^2}{2\hbar^2\tau}\right]. \quad (2.9)$$

The approximate expression for the many-body density matrix given in Eq. 2.8 becomes exact in the limit $P \rightarrow \infty$ (i.e. $\tau \rightarrow 0$). Upon substituting this expression into Eq. 2.3, an exact expression for the thermal expectation value is obtained [29], which is of the form

$$\langle \hat{\mathcal{A}} \rangle = \frac{\int \mathcal{D}R(\tau) \mathcal{A}(R(\tau)) \exp\{-\mathcal{S}[R(\tau)]\}}{\int \mathcal{D}R(\tau) \exp\{-\mathcal{S}[R(\tau)]\}}, \quad (2.10)$$

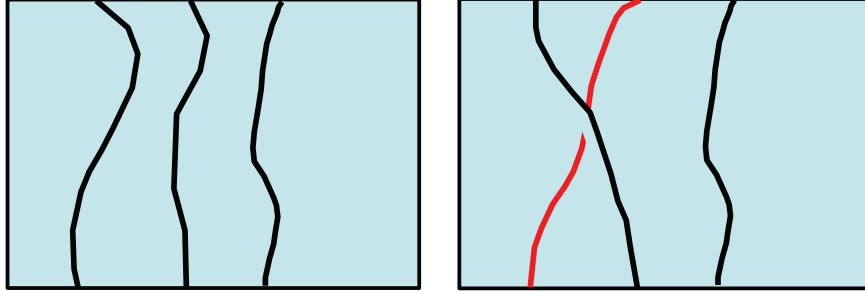


Figure 2.1: Permutation sampling in conventional PIMC

where the integral is over all continuous many-particle “path” $R(\tau)$ in the interval $0 \leq \tau \leq \beta$ and $R(\beta) = R(0)$. $\mathcal{S}[R(\tau)]$ is the Euclidean action given by

$$\mathcal{S}[R(u)] = \int_0^\beta du \left\{ \sum_{i=1}^N \frac{m}{2\hbar^2} \left(\frac{d\mathbf{r}_i}{du} \right)^2 + \mathcal{V}(R(u)) \right\}. \quad (2.11)$$

2.B.2 Quantum Statistics

The above formalism can be used to compute the thermodynamics properties of systems assuming the molecules are distinguishable, but our system of interest only focus on indistinguishable Bose particles obeying Bose statistics. However, we have to take into account the Bosonic character in order to ensure that the many-body density matrix have proper symmetry when particle labels interchange. To ensure this, the many-body paths must terminate at $\tau = \beta$ having the same position for all the particles at $\tau = 0$ with possible permutation of labels of the particles, i.e., $R(\beta) = \mathcal{P}R(0)$, where \mathcal{P} is a permutation of particle indices. Such permutations underlie phenomena such as Bose-Einstein condensation and superfluidity [30].

2.B.3 Conventional PIMC Permutation Sampling

Permutation sampling of many-particle paths is very crucial in Monte Carlo simulations. The conventional PIMC permutation sampling developed by Ceperley [30] is realized through elementary moves that modify portions of single-particle in a closed (β -periodic) paths. Permutation cycles consisting of many-particles are sampled by cutting and reconnecting pairs of world lines in such a way that permutations occur while still in the diagonal sector, Fig. 2.1 illustrates this. The sampling efficiency of this scheme is reasonable if particles interact weakly. However, it is inefficient when particles interact through a repulsive, hard core potentials which results from the reconstruction of world-line segment involving bringing two or more particles close to one another leading to a high potential energy. Such permutations will result in low acceptance rate which is a serious problem when permutation exchanges involves more than two particles. The observation of phenomenon such as superfluidity is affected by this inefficiency, which involves long permutation cycles of particles in the system.

2.B.4 Permutation Sampling In Worm Algorithm

The flaws in the conventional PIMC is completely overcome in Worm Algorithm. The Worm Algorithm differs from the conventional PIMC in terms of the configuration space. Worm Algorithm operates on an extended configurational space, which includes the closed world-line configuration, also known as Z-sector and the open world-line configuration (worm), also called G-sector. The Z-sector configuration are diagonal, thereby contributing to the partition function, the reverse is the case in the G-sector configuration, contributing

only to one-particle *Matsubara Green Function*, given by

$$G(\mathbf{r}_1, \mathbf{r}_2, \tau) = -\langle \hat{\mathcal{T}}[\hat{\psi}(\mathbf{r}_2, \tau)\hat{\psi}^\dagger(\mathbf{r}_1, \tau = 0)] \rangle, \quad (2.12)$$

where $\hat{\mathcal{T}}$ is the time ordering operator, $-\beta \leq \tau \leq \beta$, $\hat{\psi}^\dagger$ and $\hat{\psi}$ are time-dependent Bose field operators. The zero-time limit of the one-particle Matsubara Green function gives a one-particle density matrix, $n(\mathbf{r}_2, \mathbf{r}_1)$, from which we can compute the momentum distribution [31] directly in the continuous-space Worm Algorithm. The worm in the G-sector configuration have two dangling ends which are known as Ira (head) and Masha (tail). Sampling of configuration occurs through simple set of local update all involving Ira and Masha.

Worm Algorithm is currently one of the powerful methodology to study thermodynamic properties of quantum-mechanical systems comprising of many interacting particles. The Worm Algorithm can be carried out in either a canonical or grand-canonical ensemble, the latter resulting from fluctuations of particle number through creation and annihilation of worms. In our present implementation, the Z-sector configuration, have a fixed N number of particles, while the G-sector configuration have a single worm and $N - 1$ particle world lines.

2.B.5 Thermodynamic Estimators and Statistical Errors Evaluation

In this study, we compute thermodynamic properties such as; energetics, global superfluid fraction, $\rho_s(T)$, the local radial superfluid density, $n_s(r)$ and

the total radial density, $n(r)$. The energetics were obtained using the energy estimator, extensively discussed in Ref. [32]. The average Kinetic energy is given by

$$\langle K \rangle \approx \frac{3}{2\tau} - \frac{1}{4\lambda\tau^2} \langle (\mathbf{r}_l - \mathbf{r}_{l+1})^2 \rangle + \frac{\lambda\tau^2}{9} \langle (\nabla\mathcal{V}(\mathbf{R}_{2l}))^2 \rangle, \quad (2.13)$$

where $\langle \dots \rangle$ represents the thermal average, $(\mathbf{r}_l - \mathbf{r}_{l+1})^2$ is the square of the distance between two *beads* along a world line, and the gradient of the potential energy \mathcal{V} is taken with respect to the coordinate of one of the particles at an even time slice. The expression for the average potential energy per particle is given by

$$\langle \mathcal{V} \rangle \approx \frac{1}{N} \langle \mathcal{V}(\mathbf{R}_{2l-1}) \rangle. \quad (2.14)$$

We estimated the superfluid fraction using the well-known “area” estimator [33]. The superfluid fraction of a finite system, defined as the fraction that decouples from an externally induced rotation is expressed as

$$\rho_S(T) = \frac{4m^2T}{\hbar^2 I_c} \langle A^2 \rangle, \quad (2.15)$$

where I_c is the classical moment of inertia and A is the total area covered by the many-particle paths, projected to a perpendicular plane of one of the three identical rotation axes.

The radial superfluid density was computed by means of a microscopic estimator proposed by Kwon *et al.* [56], the local superfluid density, $n_s(r)$, is given by

$$\frac{n_s(r)}{n(r)} = \frac{4m^2 \langle AA(r) \rangle}{\beta \hbar^2 I_c(r)}, \quad (2.16)$$

where $A(r)$ and $I_c(r)$ are contributions from A and I_c respectively, computed from a spherical shell of radius r centered at the center of mass of the cluster.

The thermal average of a physical observable $\hat{\mathcal{A}}$ is known to be calculated from the average of its value over a large set of N_r samples X_j generated through sampling procedure, as

$$\langle \hat{\mathcal{A}} \rangle \approx \frac{1}{N_r} \sum_{j=1}^{N_r} \mathcal{A}(\mathbf{X}_j). \quad (2.17)$$

The computation of statistical errors for our calculated expectation values is very crucial as it makes our calculations more meaningful. For an independent and normally distributed values $\mathcal{A}(\mathbf{X}_j)$, the error estimate on $\langle \hat{\mathcal{A}} \rangle$ can be estimated as

$$\sigma \approx \sqrt{\frac{\sum_{j=1}^{N_r} (\mathcal{A}(\mathbf{X}_j) - \langle \mathcal{A} \rangle)^2}{(N_r - 1)}}. \quad (2.18)$$

However, our sample states are generated via Markov chain in which one state is generated by visiting the previous one. Successive state in this random walk are correlated and the statistical errors are being underestimated using Eq. 2.18. One must find another means to perform the average over uncorrelated configurations. An alternate approach is to spilt the simulation up into a number of equal blocks containing a large (thousand) number of successive configurations, over which partial averages for each block are calculated and stored. A bin is then constructed for a fixed number of blocks in each, and the error is thus obtained as the standard deviation of the resulting histogram. We refer the reader to Ref. [34], for more detailed procedure for estimating the standard error which we utilized in the work.

Chapter 3

SYSTEMATICS OF SMALL PARA-HYDROGEN CLUSTERS IN TWO DIMENSIONS

In this chapter, we discuss the properties of two-dimensional properties of parahydrogen clusters comprising between $N = 7$ and $N = 30$ molecules at $T = 0.25\text{K}$.¹

3.A Introduction

The physics of small parahydrogen clusters remains a subject of current interest, mainly because this system features a rather unique interplay of clas-

¹A version of this chapter has been published as:
Saheed Idowu and Massimo Boninsegni. *Journal of Chemical Physics* **140**, 204310 (2014).

sical and quantum physics [35]. Due to its low mass and bosonic character, parahydrogen ($p\text{-H}_2$) was predicted a long time ago to undergo a superfluid transition, at temperature $T \lesssim 6$ K [36]. However, the equilibrium phase of bulk $p\text{-H}_2$ in the $T \rightarrow 0$ limit is a crystal, even in reduced dimensions [37, 38], due to the depth of the attractive well of the interaction potential between two hydrogen molecules. The theoretical suggestion that a liquidlike phase of $p\text{-H}_2$ could be stabilized in two dimensions (2D) by an underlying impurity substrate [39] is not supported by several recent calculations [40, 41].

There is experimental proof, on the other hand, that small clusters of $p\text{-H}_2$ in three dimensions can escape crystallization [42], down to a temperature sufficiently low that a finite superfluid response, defined as the dissipationless rotation about an axis going through the center of mass, is theoretically predicted to arise in the nanoscale clusters ($\lesssim 30$ molecules) at a temperature of the order of a few tenths of a K [43, 44, 45]. While most of these clusters are expected to remain essentially liquidlike, i.e., structureless, all the way to zero temperature, in some cases undergoing quantum melting at sufficiently low T , $(p\text{-H}_2)_{26}$ is predicted to retain some well-defined structural short-range order, even with the concurrent development of superfluid coherence at low T , behaving in some sense as a finite-size “supersolid” [46].

An interesting question is what happens if clusters are themselves confined to 2D, which could be achieved experimentally by adsorbing $p\text{-H}_2$ on a suitable substrate, strong enough to confine molecules effectively to 2D, but also weak enough to allow for the neglect of corrugation. Substrates of alkali metals might be a good candidate [47], but progress toward the stabilization of quasi-2D H_2 clusters on a different type of substrate has been recently reported [21]. Reduction of dimensionality brings about two competing effects. On the one

hand, the lower coordination number is expected to weaken the tendency of the system to crystallize, but also has the effect of hindering quantum-mechanical exchanges of identical particles, which have been shown to play a crucial role in the stabilization of a liquidlike structure at low T [44, 45].

The only existing theoretical study of p -H₂ clusters in 2D is that by Gordillo and Ceperley, who carried out first principles Path Integral Monte Carlo simulations, down to $T = 0.3$ K [15]. Their main physical findings were that clusters comprising at the most two concentric shells of molecules around the center of mass (typically ten molecules or less) are essentially structureless, i.e., liquidlike, and superfluid at low T ($\lesssim 1$ K); as more molecules are added to the cluster, a solidlike core starts forming, with the concomitant, gradual suppression of the superfluid response. From this observation, the authors inferred that, as cluster size is increased, superfluidity is progressively confined to a liquidlike outer shell, while the solidlike core is insulating.

In this work, we present results of Quantum Monte Carlo simulations of two dimensional p -H₂ clusters of size ranging from $N = 7$ to $N = 30$ molecules, in the temperature range $0.25 \leq T \leq 1$ K. We computed energetic and superfluid properties of the clusters, and investigated their structure by means of density profiles computed with respect to the center of mass of the cluster, as well as through actual density maps, affording direct visual insight in 2D.

In general, our estimates for the energy per particle are in satisfactory quantitative agreement with those of Ref. [15], on taking into account the statistical uncertainties of both calculations; on the other hand, we obtain a stronger superfluid signal than they do, especially for clusters with more than ~ 10 molecules. Indeed, we find a robust superfluid signal at the lowest temperature considered here, for clusters comprising as many as $N = 25$ p -H₂

molecules; analogously to what found in 3D clusters, the dependence of the superfluid response on N is non-monotonic [44, 45].

More importantly, the physical picture that emerges from our study is qualitatively different from that of Ref. [15] in a number of relevant aspects. First and foremost, none of the clusters studied here can be regarded as truly “liquidlike”, at low T . In particular, our radial density profiles for the smaller clusters are quantitatively very different from those of Ref. [15], featuring much higher peaks, separated in turn by much shallower dips. This is indicative of a well-defined structure, in which molecules tend to occupy preferred lattice sites, something that is confirmed by our computed density maps. Second, the calculation of the local superfluid density shows that in all superfluid clusters the response is not confined at the surface but rather uniform throughout the system, much like in three-dimensional (3D) clusters [48]. Thus, no meaningful distinction can be drawn between a non-superfluid, solidlike center, and a superfluid liquidlike outer part, for any of the superfluid clusters; rather, they should be regarded as featuring concurrently superfluid and solidlike properties. In this sense, these small 2D clusters may be regarded as naturally occurring nanoscale “supersolids”.

In the next section, we describe the microscopic model underlying this calculation and furnish basic computational details. A thorough illustration of our results is provided in Sec. 3.C. In Sec. 3.D, we discuss the physical conclusions and also provide possible scenarios of stabilizing bulk superfluid phase of p -H₂ in two dimensions.

3.B Model And Methodology

In this chapter, our system of interest is modeled as a collection of N parahydrogen ($p\text{-H}_2$) molecules, regarded as point particles, moving in two physical dimensions. The quantum mechanical many-body Hamiltonian is the same as in Ref. [15], given by

$$\hat{H} = -\lambda \sum_{i=1}^N \nabla_i^2 + V(R), \quad (3.1)$$

where $\lambda = 12.031 \text{ K } \text{\AA}^2$, $R \equiv \mathbf{r}_1, \mathbf{r}_2, \dots, \mathbf{r}_N$ is a collective coordinate referring to all N particles in the system and $V(R)$ is the total potential energy of the configuration R , which is assumed here to be expressed as the sum of pairwise contributions, each one described by a spherical symmetric potential. In this calculation, we made use of Silvera Goldman potential [49], mostly for consistency with the calculation [50] of Ref. [15]. We estimated equilibrium thermodynamic properties of this finite system at low temperature, by means of Quantum Monte Carlo simulations, based on the Worm Algorithm in the continuous-space path integral representation.

Our simulated system is enclosed in a square cell, chosen sufficiently large to remove any effect of the boundary conditions, periodic in all directions. We use a high-temperature approximation for the imaginary time propagator accurate to fourth order [32, 53, 54] in the imaginary time step τ . The results shown here are obtained with a value of $\tau = 10^{-3} \text{ K}^{-1}$, empirically found to yield estimates indistinguishable, within our quoted statistical uncertainties, from those extrapolated to the $\tau \rightarrow 0$ limit (i.e the limit where the method becomes exact). No artificial confining potential was used in the simulation, as clusters

stay together simply as a result of the intermolecular pairwise attraction.

We compute both the global superfluid fraction ρ_S , as well as the radial, angularly averaged one, $\rho_S(r)$. We estimate the first using the well-known “area” estimator [55], the second by means of a straightforward generalization of the area estimator, applied to concentric shells of varying radii, centered at the center of mass of the cluster [56]. For the smallest clusters ($N \lesssim 10$), a more accurate estimate of the global superfluid fraction is the radial average of $\rho_S(r)$, weighted by the angularly averaged radial p -H₂ density $\rho(r)$, outside of a circle of radius $r_o \sim 2 \text{ \AA}$. This is because the statistical noise in the estimate of ρ_S arises mostly from contributions in the vicinity (i.e., within a distance r_o or less) of the center of mass.

3.C Results

As mentioned in the previous section, we carried out numerical simulation of clusters in the temperature range $0.25 \leq T \leq 1 \text{ K}$. In general, structural and energetic properties of the clusters remain unchanged below $T \sim 0.5 \text{ K}$; in particular, physical estimates reported here for $T = 0.33 \text{ K}$ or lower, should be regarded as ground state estimates, within their statistical uncertainties.

Fig. 3.1 shows the energy per molecule versus cluster size, computed at $T = 0.25 \text{ K}$. Also shown are the results reported in Ref. [15] at a slightly higher temperature ($T = 0.33 \text{ K}$). The two calculations are in excellent agreement, within their statistical uncertainties. The energy per molecule is monotonically decreasing, with no evidence of “magic numbers”, within the precision of our calculation. It attains a value around -15.3 K for a cluster with $N = 30 \text{ } p\text{-H}_2$ molecules; this is still relatively far from the 2D bulk value [37] of $\sim -23.2 \text{ K}$.

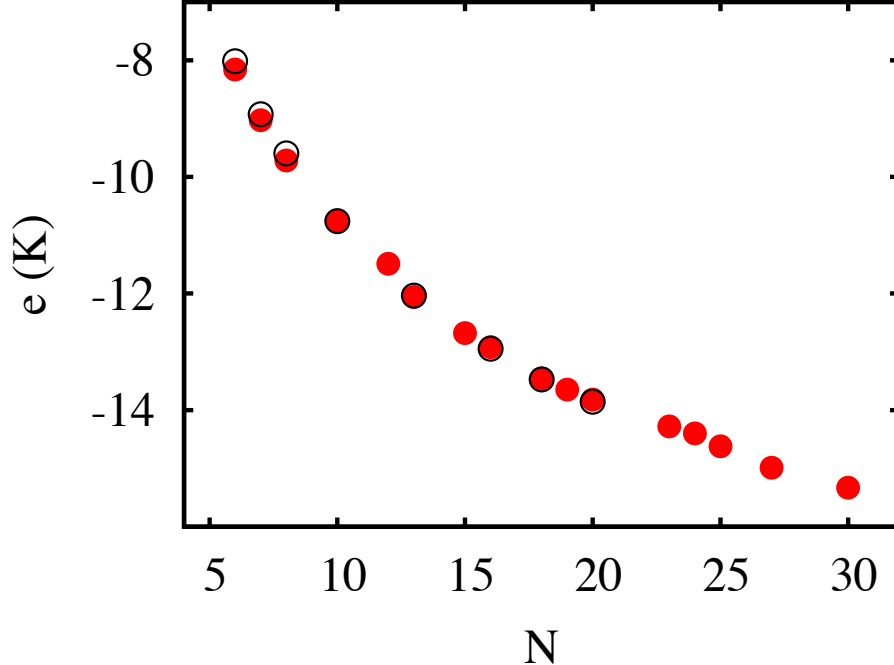


Figure 3.1: Energy per hydrogen molecule e (in K) versus cluster size N , at $T = 0.25$ K (full symbols). Also shown are the results reported in Ref. [15], at $T = 0.33$ K (open symbols). For clusters of size $N = 10, 13, 16$ and 20 , our energy estimates are indistinguishable from those of Ref. [15]. Statistical errors are at the most equal to symbol size.

In order to discuss the structural properties of the clusters, which are the main focus of this study, we begin by illustrating in some details the results for the smallest cluster studied in this work, namely that with $N = 7$ p -H₂ molecules, because in many respects this allows us to draw general conclusions, applicable to clusters of greater size as well.

Figure 3.2 shows the radial density profile $\rho(r)$ for $(p\text{-H}_2)_7$ (solid line), with respect to its center of mass, computed at a temperature $T = 0.33$ K. Two results are shown, namely that obtained in this work (solid line), and that published in Ref. [15] (filled circles); for comparison purposes, we begin by discussing the latter first. It displays two broad peaks, one at the origin,

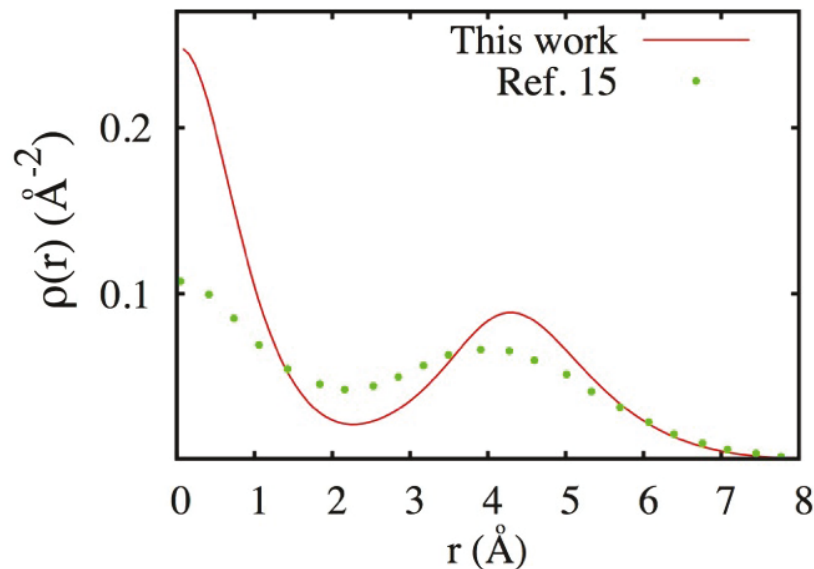


Figure 3.2: (color online) Radial density profile for a cluster with $N = 7$ p -H₂ molecules at $T = 0.33$ K (solid line). Filled circles show the corresponding result from Ref. [15]. Profiles are computed with respect to the center of mass of the cluster. Statistical errors are not visible on the scale of the figure. The local superfluid density profile for this cluster is indistinguishable from that of the local density.

signaling a particle in the center of the cluster, and an outer one, evidently the signature a floppy surrounding ring comprising the remaining six molecules. Only a minor depression between the two peaks is observed; indeed, the outer peak is barely noticeable. Such a profile was reasonably interpreted by the authors of Ref. [15] as evidence of a structureless, liquidlike cluster.

The corresponding density profile obtained in this work, on the other hand, looks distinctly different. It features two much higher and narrower peaks (the one at the origin more than twice as high with respect to that of Ref. [15]), separated by a pronounced dip, to suggest a rather sharp physical demarca-

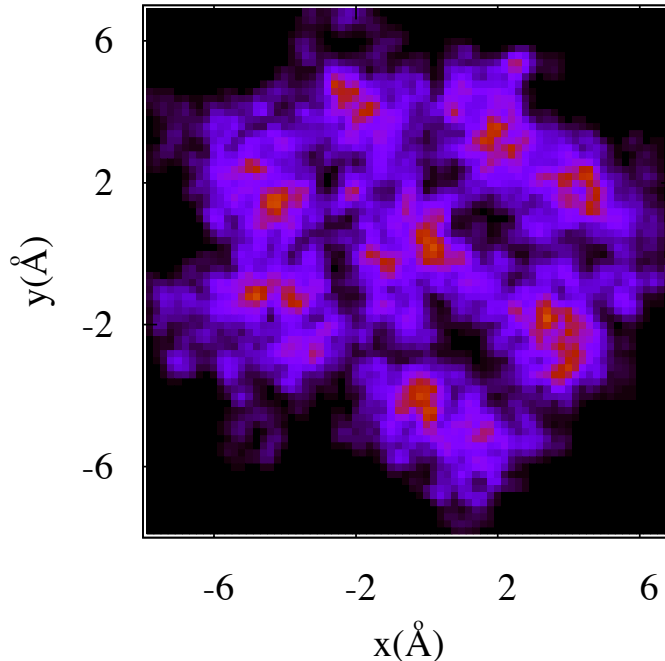


Figure 3.3: (color online) Configurational snapshot (particle world lines) yielded by a simulation of a cluster with $N = 7$ p -H₂ molecules at $T = 0.33$ K. Brighter colors correspond to a higher local density.

tion between the central particle and the surrounding ring. This points to a considerably more structured cluster, in which particles preferentially tend to be at well-defined relative positions, i.e., the cluster is solidlike [57]. The quantitative disagreement between the two results is puzzling, considering that our estimate of the energy per particle ($-8.95(2)$ K), as well as that of the superfluid fraction ρ_S ($\sim 100\%$) at this temperature are in agreement with theirs, within the statistical uncertainties of the calculations. In order to obtain an independent check of our result, we carried out a separate calculation of the ground state properties of this cluster, using the Path Integral Ground State technique [54, 58]. The details of this calculation are identical with those described in Ref. [59]. The radial density profile obtained in this second way is

identical with that at $T = 0.33$ K, given by the solid line in Fig. 3.2. This fact gives us confidence on the correctness of our results. The qualitative disagreement with the radial density profile of Ref. [15] is therefore unclear, and somewhat puzzling, at this time, as the same microscopic model is utilized.

Furthermore, In order to gain additional insight into the physics of this few-body system, we make use of the direct and visually suggestive information provided in 2D by configurational snapshots generated by the Monte Carlo simulation (see, for instance, Ref. [23]). Figure 3.3 shows a particle density map obtained from a statistically representative configuration snapshot (i.e., particle world lines) for the cluster under exam, at the same temperature as in Fig 3.2. By “statistically” representative, it is meant here that every configuration generated in the simulation is roughly similar to that shown in the Figure, differing from it mostly by a mere rotation. Albeit smeared by zero point motion, lumps associated to individual molecules are clearly identifiable, forming an ordered structure, with a visible gap between the particle in middle of the cluster and those in the outer ring. In spite of this relatively “ordered” arrangement, in turn implying a degree of molecular localization, exchanges of indistinguishable particles occur frequently, hence large superfluid response. Indeed, the probability for a single-particle world line not too close onto itself, meaning that the particle participates to a cycle of exchange with one or more partners, is as large as 30%.

The superfluid fraction of this droplet is, as mentioned above, 100% at $T \leq 0.33$ K, within statistical uncertainty. Moreover, the superfluid signal is uniformly distributed throughout the whole cluster, not concentrated at any specific region (e.g., the surface); in fact, the computed angularly averaged, local superfluid density profile is indistinguishable from that of the local den-

sity, shown in Fig. 3.2. This is much like already observed in 3D clusters [48]. Thus, the two seemingly exclusive superfluid and solidlike properties appear to merge into a single, remarkable “supersolid phase” [57].

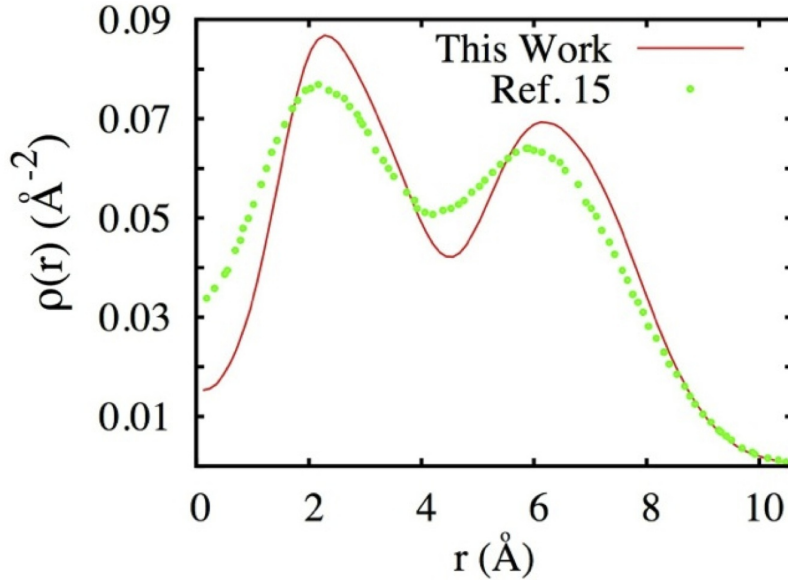


Figure 3.4: (color online) Radial density profile for cluster with $N = 13$ at $T = 0.33$ K (solid line). Also shown is the corresponding result from Ref. [15] (filled circles). Profiles are computed with respect to the center of mass of the cluster. Statistical errors are not visible on the scale of the figure.

The structural short-range order characterizing this small cluster is found to be the same in *all* other clusters investigated here. All of them are solidlike, in no case quantum-mechanical exchanges causing the melting at low T into a featureless, liquidlike cluster, an effect which is also observed in simulations of 3D clusters, in this temperature range [44, 45]. Figures 3.4 and 3.5 show radial density profiles for clusters with $N = 13$ and 20 molecules, at $T = 0.33$ K. Comparison with Ref. [15] again shows considerably more structure in the sim-

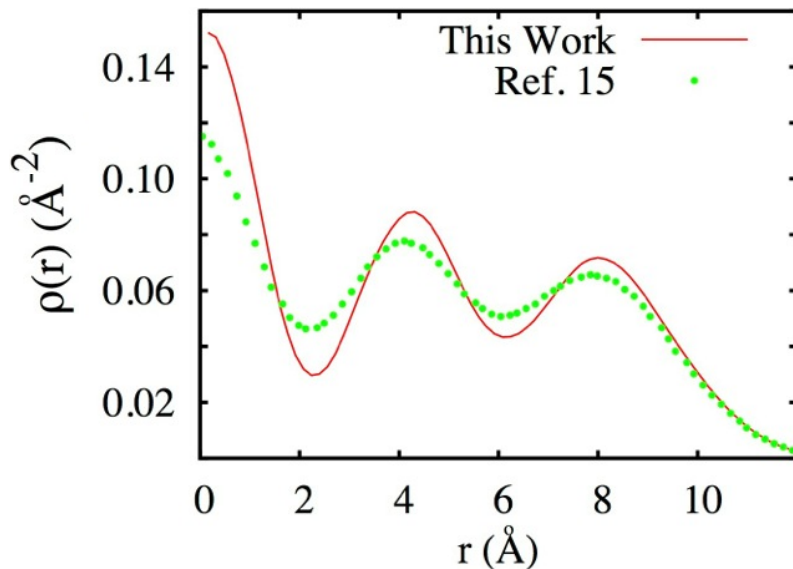


Figure 3.5: (color online) Radial density profile for cluster with $N = 20$ at $T = 0.33$ K (solid line). Also shown is the corresponding result from Ref. [15] (filled circles). Profiles are computed with respect to the center of mass of the cluster. Statistical errors are not visible on the scale of the figure.

ulations carried out here. As the size is increased, both studies yield evidence of greater structural short-range order, but quantitative differences between radial density profiles remain visible even for the largest cluster studied in Ref. [15], i.e., that with $N = 20$ (Fig. 3.5). While a quantitative characterization of particle localization in these clusters might be obtained by making use of estimators proposed in Refs. [60, 61, 62], nonetheless our results, consistently yield higher peaks and more pronounced dips in between, i.e., a significantly more rigid, solidlike structure. This is in marked quantitative, and for the smallest clusters even *qualitative* disagreement with the physical conclusions of Ref. [15].

We now discuss the superfluid properties of the few-body system. For all

clusters with $N \leq 23$, the superfluid fraction ρ_s is indistinguishable from 100% within statistical uncertainties at $T = 0.25$ K. Our superfluid signal is stronger than that reported in Ref. [15] for clusters with $N = 13, 16$ and 20 , for all of which they find is worth 0.6 ± 0.1 at $T = 0.33$ K, whereas for these four specific clusters we find values in excess of 90% at that same temperature. The largest cluster for which a significantly large superfluid response is observed at the lowest temperature considered here, namely $T = 0.25$ K, comprises 25 molecules; its superfluid fraction is again worth approximately 100% at $T = 0.25$ K.

The superfluid response is observed to drop abruptly for $N > 25$; indeed, for none of the clusters with $26 \leq N \leq 30$ could we obtain an appreciable value of ρ_S in this study [63], at the lowest temperature considered here. It should be noted, however, that the dependence of ρ_S on N for a fixed low T is not monotonic, a fact which have been observed in 3D clusters [44, 45] with $22 \lesssim N \lesssim 30$. In particular, at $T = 0.25$ K, ρ_S is observed to drop down to level of statistical noise for a cluster with $N = 24$, to rebound to $\sim 100\%$ on adding a single molecules (i.e., for a cluster with $N = 25$), to drop again to zero if another molecule is added.

Such an intriguing behaviour, most remarkably mimicking what observed in 3D clusters with the same numbers of molecules, cannot be straightforwardly related to the shape of the cluster, and/or to the completion of any regular geometrical structure, occurring on adding a molecule to (or removing one from) a cluster with $N = 25$, nor to some greater “liquidlike” character of the $N = 25$ system. In Fig. 3.6, we compare the density profiles of two clusters with $N = 25$ and 26 p -H₂ molecules at $T = 0.25$ K, at which the cluster with 25 molecules is entirely superfluid, and that with 26 features no measurable

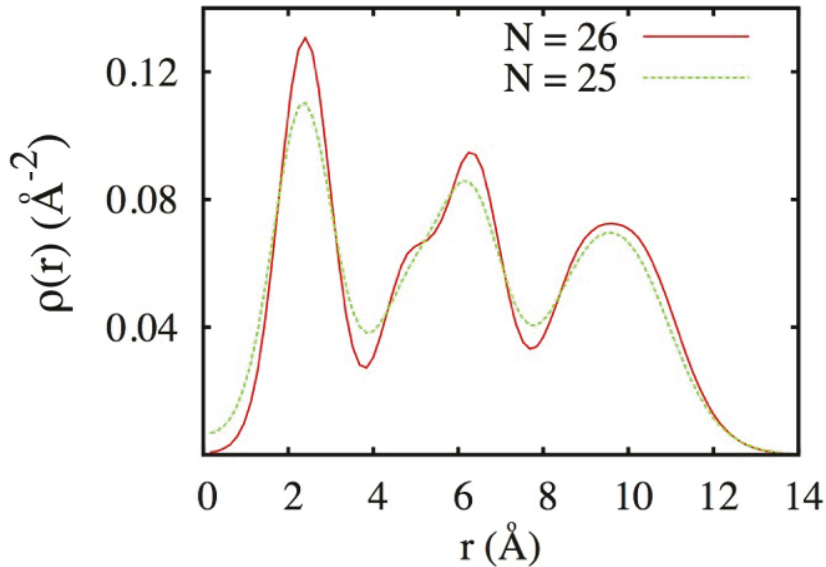


Figure 3.6: (color online) Radial density profiles for clusters with $N = 25$ (dashed line) and 26 (solid line) p -H₂ molecules at $T = 0.25$ K. Profiles are computed with respect to the center of mass of the cluster. Statistical errors are not visible on the scale of the figure.

superfluid response. Both profiles show three peaks, i.e., three concentric shells, but that of the the cluster with one extra molecule is noticeably more structured, and its first two peaks sharper. On the other hand, the peak corresponding to the outer shell is rather smooth, very similar in both cases. Thus, the main structural difference between the two clusters seems to be that the non-superfluid one has enhanced solid order in the two inner shells. This observation, together with the fact that the superfluid response is uniformly distributed throughout the cluster, in turn undermines the suggestion that superfluidity should correlate with the presence of a liquidlike outer shell, of which no evidence is shown by the representative configuration snapshots of figures 3.7 and 3.8. Indeed, both clusters display a rather ordered structure,

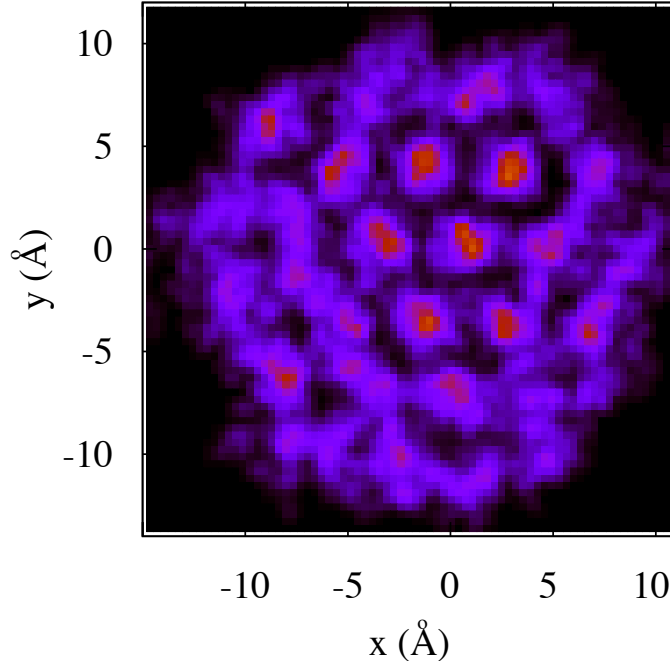


Figure 3.7: (color online) Configurational snapshot (particle world lines) yielded by a simulation of a cluster with $N = 25$ $p\text{-H}_2$ molecules at $T = 0.25$ K. Brighter colors correspond to a higher local density.

although the molecules sitting at the surface are obviously less bound.

3.D Discussion

In this chapter, we have performed a systematic investigation of the low temperature properties of small clusters of $p\text{-H}_2$ in two dimensions, using first principle quantum Monte Carlo simulations, whose only input is the intermolecular pair potential. Some of the physical properties of these clusters are very similar to those of clusters in three dimensions. For example, the non-monotonic dependence of the superfluid response at low temperature on the number N of molecules in the cluster, is also observed in the 3D system. There too, most notably, the numbers $N = 25$ and 26 are associated with

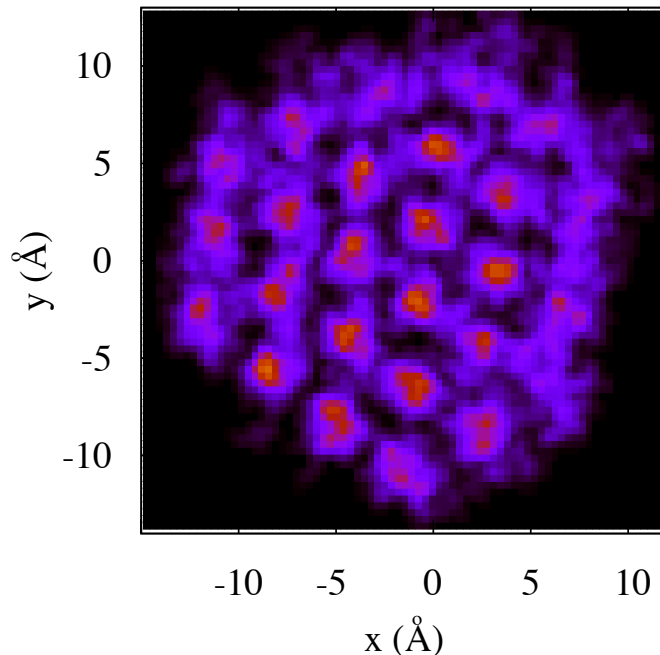


Figure 3.8: (color online) Configurational snapshot (particle world lines) yielded by a simulation of a cluster with $N = 26$ p -H₂ molecules at $T = 0.25$ K. Brighter colors correspond to a higher local density.

the same effect observed here, i.e., the drop of the superfluid fraction from nearly 100% to a value close to zero (in the temperature range considered here), on adding a single molecule to the $N=25$ cluster. This suggests that a significant compensating effect takes place on reducing dimensionality; the enhancement of quantum fluctuations, and the concomitant suppression of quantum-mechanical exchanges (due to the confinement of molecular motion to a plane, and the hard, repulsive core of the intermolecular potential at short distances) both contribute to preserve some of the same physics observed in three dimensions.

Additionally, some of the features of 2D p -H₂ droplets set them aside from their 3D counterpart. The most striking feature of these few-body systems, is

the simultaneous presence of what can be reasonably described as short-range order, whereby molecules tend to form specific geometrical arrangements, typically resulting from a classical mechanism (i.e., minimization of potential energy), and a finite superfluid response, originating from exchanges of identical molecules. Much like in the 3D case, superfluidity is underlain by cycles of exchanges involving all of the molecules, not just those on the outer shell. Indeed, the participation of inner molecules to exchanges is crucial, witness the fact that as the number N is increased beyond 25, at which point clusters are no longer superfluid at the lowest temperature observed, their inner structure concurrently appears much more rigid (as shown by the comparison in Fig. 3.6), consistently with inner molecules to be more localized and are less involved in exchanges.

What are the implications of this study, if any, can be deduced from the results of this study, regarding a possible stabilization of a superfluid phase of bulk p -H₂? The suggestion that one might be able to use frustration, either arising from disorder [41, 64] or from an underlying impurity substrate incommensurate with the equilibrium triangular crystalline phase of p -H₂ in two dimension [39], has not been shown to lead to a superfluid phase, although recently renewed claims to that effect have been made [65].

Also, one could consider borrowing on ideas arising from theoretical studies of superfluidity (and supersolidity) in cold atom assemblies [66]. In particular, one could imagine patterning a suitably chosen surface with regularly arranged adsorption sites (e.g., on a triangular lattice). Each site could be designed to accommodate a number of p -H₂ molecules between, say, ten and twenty, acting in a sense as a “molecular quantum dots”, turning superfluid at low T . Conceivably, upon choosing the lattice constant of the adsorption lattice suitably,

it might be possible to establish phase coherence throughout the whole system, through the tunnelling of individual p -H₂ molecules across adjacent adsorption wells. The ensuing superfluid phase would be similar to the supersolid droplet crystal phase of Refs. [67] and [14], with the important conceptual difference that in the present case the adsorption lattice is externally imposed, as opposed to arising from inter-particle interactions. This scenario is discussed in the next chapter.

Chapter 4

SUPERFLUID RESPONSE OF 2D PARAHYDROGEN CLUSTERS IN CONFINEMENT

4.A Introduction

In this chapter, we will discuss in great detail the effect of confinement on the superfluid properties of small 2D p -H₂ clusters. We will also discuss the results obtained on possible stabilization of a bulk 2D superfluid phase of p -H₂, where a global superfluid response would arise from tunnelling of molecules across adjacent unit cells.¹

¹A version of this chapter has been published as:
Saheed Idowu and Massimo Boninsegni. *Journal of Chemical Physics* **142**, 134303 (2015).

4.B Results

4.B.1 Superfluidity

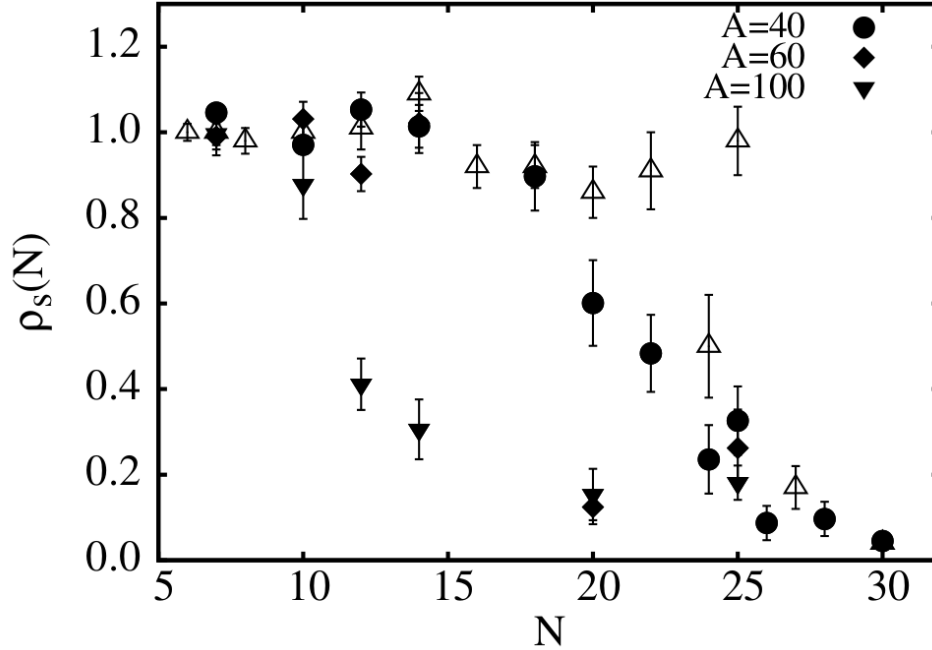


Figure 4.1: Superfluid fraction of 2D p -H₂ clusters confined in a Gaussian well of size $\sigma = 3 \text{ \AA}$ and depth $A = 40 \text{ K}$ (circles), $A = 60 \text{ K}$ (diamonds) and $A = 100 \text{ K}$ (triangles), at a temperature $T = 0.25 \text{ K}$. Open triangles show results for free clusters. When not shown, statistical errors are at the most equal to symbol size.

We start the illustration of the results of our study for clusters trapped inside a well of size $\sigma = 3 \text{ \AA}$ i.e., roughly the radius of the inner shell of the clusters [20]. Figure 4.1 shows the superfluid fraction $\rho_s(N)$ at a temperature $T = 0.25 \text{ K}$, for clusters comprising up to $N = 30$ molecules, for wells of depth $A = 40, 60$ and 100 K respectively. Also shown are the corresponding results for free clusters (i.e., $A = 0$), from Ref. [20].

As discussed therein, a rather sharp demarcation exists for free clusters,

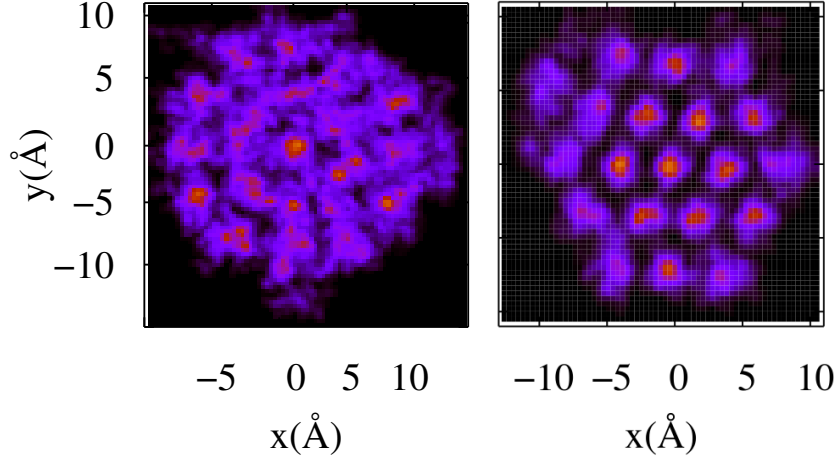


Figure 4.2: Configurational snapshots (particle world lines) yielded by a simulation of a cluster with $N = 20$ p -H₂ molecules at $T = 0.25$ K. *Left*: Free cluster. *Right*: Cluster confined inside a gaussian well of depth $A = 100$ K and size $\sigma = 3$ Å. Brighter colors correspond to a higher local density.

in terms of superfluid response. For, those with less than 26 molecules are essentially 100% superfluid at this low T (with the sole anomaly of $N = 24$ for which the superfluid response is approximately one half), whereas the superfluid response is suppressed in larger clusters.

For a relatively shallow well ($A \sim 20$ K), the superfluid response of the confined clusters remains close (within $\sim 10\%$) to that of the free ones. As the depth of the confining well is increased, superfluidity is gradually suppressed, but the smallest clusters, namely those with $N \lesssim 15$, retain their superfluid properties (those with $N \lesssim 10$ essentially entirely), even for the deepest well considered here, namely with $A = 100$ K. As shown in Fig. 4.1, clusters whose superfluid response is most significantly affected by confinement are the largest ones, i.e., those with $N \gtrsim 18$.

This result may seem counterintuitive, as one might expect confinement to have a more disruptive effect on the superfluidity of smaller clusters. The

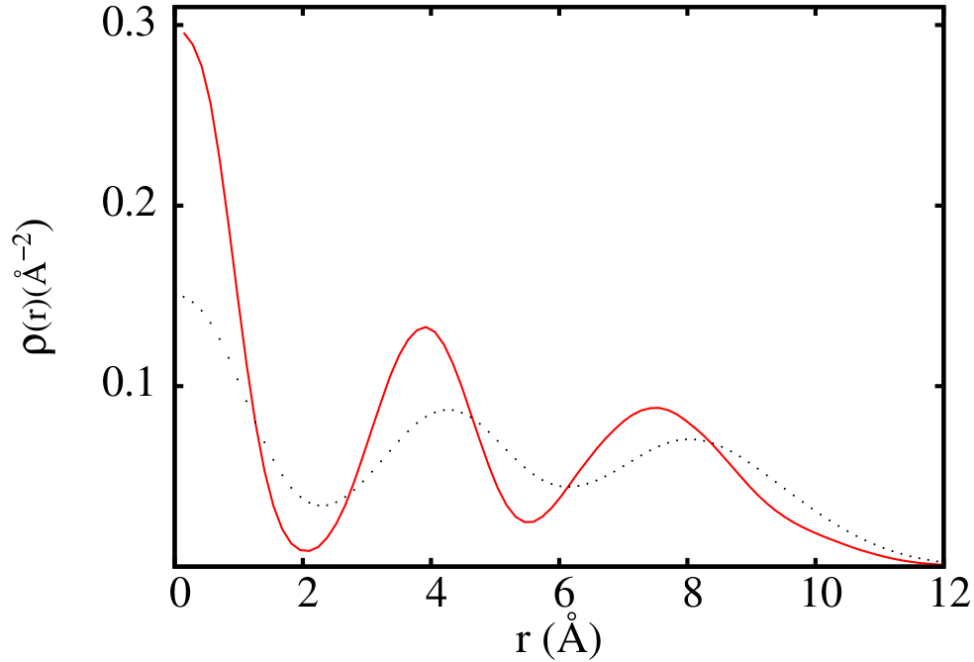


Figure 4.3: Radial density profile for a cluster of $N = 20$ p -H₂ molecules, confined in a Gaussian well of size $\sigma = 3$ Å and of depth $A = 100$ K. Dotted line shows the corresponding profile for a free clusters. These profiles are computed at $T = 0.25$ K. Statistical errors are not visible on the scale of the figure.

reasoning would be that, as the well depth is increased, the molecules in the inner part of the cluster become localized, with the ensuing suppression of quantum exchanges, and thus of superfluidity, which might remain confined to the outer region of a larger cluster, where molecules enjoy greater mobility and where the effect of the confining potential is weak, for a well of size 3 Å.

This is certainly what happens, as qualitatively shown in Fig. 4.2 for a cluster with $N = 20$ molecules. Configurational snapshots for a free cluster (left), and one trapped inside a well of depth $A = 100$ K (right), clearly show a much greater localization of molecules in the center of the cluster; this is more quantitatively illustrated by the radial density profile, computed with respect

to the center of the well, shown in Fig. 4.3. Exchanges of p -H₂ molecules in the center of such a deep well is rare. Exchanges still occur in the outer shell, but superfluidity is nonetheless suppressed to statistical noise level in the confined cluster, while it is nearly 100% in the free cluster. This is consistent with the notion that superfluidity in p -H₂ clusters, which have a strong “solid-like” structure, crucially hinges on exchanges of molecules across different shells, an effect already noticed in 3D clusters [48]. In the presence of a confining well, superfluidity is resilient in smaller clusters, consisting of essentially only one shell, because molecules are less compressed than in the case of clusters with an additional shell, and therefore enjoy sufficient mobility, even for fairly deep wells (~ 100 K). Figure 4.4 shows $\rho_S(N)$ for the same clusters as in Fig. 4.1, but for a well of size $\sigma = 6$ Å. The results are qualitatively similar to those obtained for a tighter well, the suppression of superfluidity being more noticeable in this case, especially for clusters comprising between 15 and 20 molecules, for a well of the same depth. In this case, the confining potential is most rapidly varying roughly between the first and the second shell, for clusters of more than ~ 15 molecules, which has a greater suppressing effect for intershell exchanges. The superfluid response of clusters of 15 molecules or less, on the other hand, is relatively unaffected for depths up to 60 K. If the characteristic radius of the well is further increased, essentially beyond that of the cluster itself, confinement becomes increasingly irrelevant, understandably.

The main physical conclusion of this part of our study is that the superfluid response of 2D p -H₂ clusters of less than $\lesssim 20$ molecules is quantitatively rather robust against confinement. This is a direct consequence of the “super-solid” character of these clusters, which renders them less compressible than liquid-like ones, consequently protecting their main physical properties from

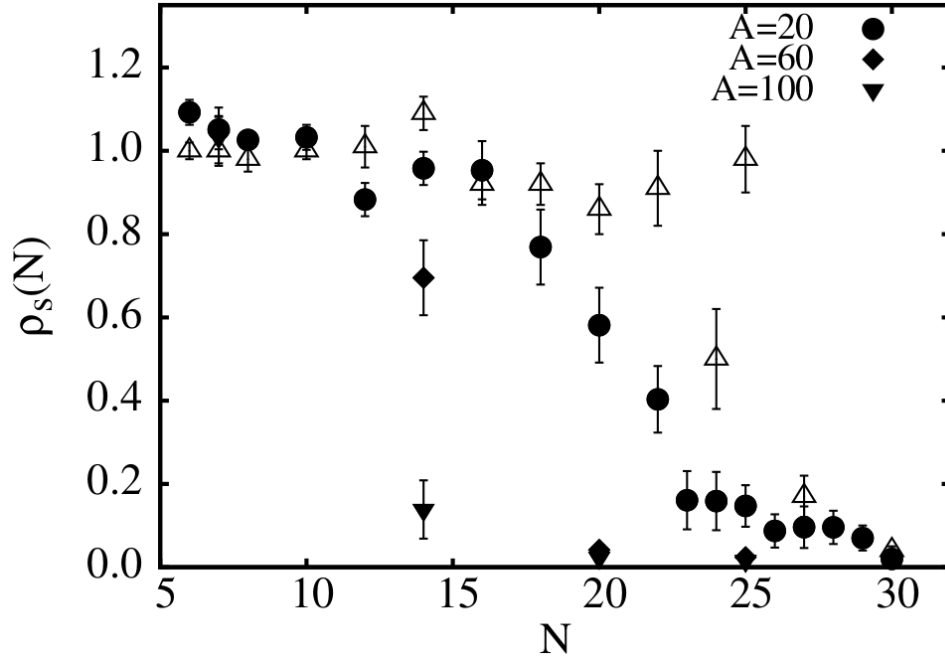


Figure 4.4: Superfluid fraction of 2D p -H₂ clusters confined in a Gaussian well of size $\sigma = 6 \text{ \AA}$ and depth $A = 20 \text{ K}$ (circles), $A = 60 \text{ K}$ (diamonds) and $A = 100 \text{ K}$ (triangles), at a temperature $T = 0.25 \text{ K}$. Open triangles show results for free clusters. When not shown, statistical errors are at the most equal to symbol size.

the influence of external agents. The basic physics of the superfluid clusters in confinement quantitatively reproduces that of the free clusters.

4.B.2 Energetics

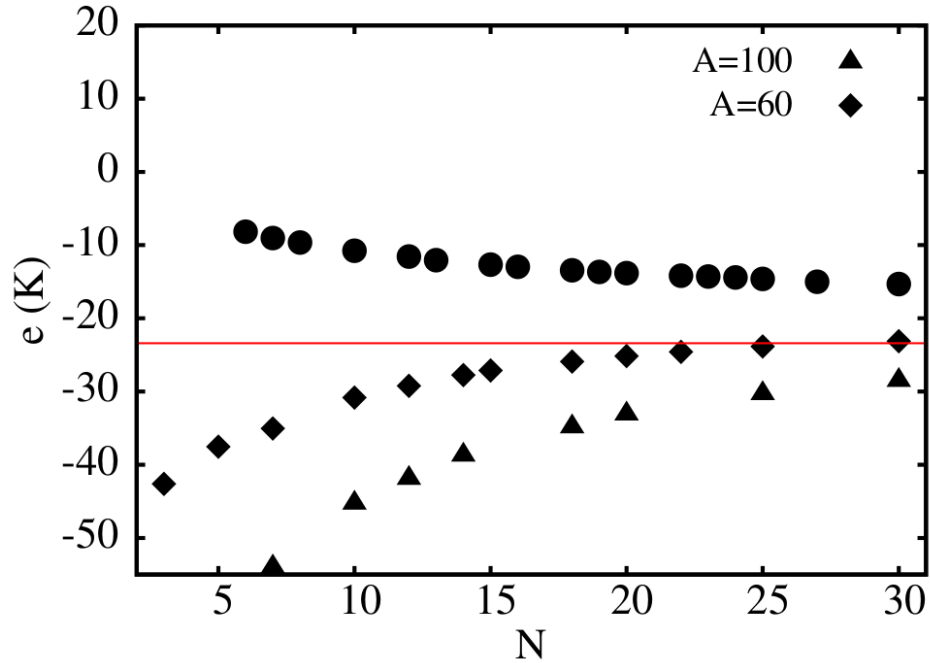


Figure 4.5: Energy per p -H₂ molecule for clusters of N molecules ($1 \leq N \leq 30$), trapped in a well of size $\sigma = 3 \text{ \AA}$ and depth $A = 60 \text{ K}$ (diamonds) and $A = 100 \text{ K}$ (triangles). Circles show the corresponding values for free clusters (i.e., $A = 0$). Statistical errors are smaller than symbol size. Horizontal line refers to the ground state energy per molecule of bulk p -H₂ in its 2D crystal equilibrium phase.

The energetics of the confined clusters remains a goal of interest in view of the possible stabilization of a crystal of 2D clusters, turning superfluid at low temperature, as explained in the Introduction of this chapter. Fig. 4.5 shows a typical results for the energy per molecule in a cluster comprising up to thirty molecules, confined in a Gaussian well of varying amplitude and size

$\sigma = 3 \text{ \AA}$. The qualitative behaviour observed in a well of twice the size is the same, all curves being shifted downward.

The idea is that of “pinning” small $p\text{-H}_2$ clusters at the sites of a triangular lattice whose lattice constant d should be of the order of, or not much greater than, the characteristic size of a superfluid cluster, in order to allow for tunnelling of outer shell molecules across adjacent sites. The results shown here and in Ref. [20] suggest that $d \sim 20 \text{ \AA}$.

Let us assume for definiteness a number of molecules per unit cell N equal to 20, yielding a 2D density for the cluster crystal of approximately 0.058 \AA^{-2} . This is significantly less than the ground state equilibrium density of $p\text{-H}_2$ in 2D, equal to [37] $\rho_0 = 0.0667 \text{ \AA}^{-2}$, at which the system is a non-superfluid crystal with one particle per unit cell; the energy per molecule in such a phase is $\epsilon_0 = -23.4 \text{ K}$. In order for the low density cluster crystal phase to be energetically stable against the formation of the ordinary 2D crystal of density ρ_0 , the energy per $p\text{-H}_2$ molecule should be lower than $\epsilon_0 + \Delta$, Δ being the average potential energy in a lattice of identical wells, of a given lattice constant d . This quantity can be easily computed numerically.

From Fig. 4.3, we see that the radius of a cluster with 20 molecules is $\sim 12 \text{ \AA}$. If the lattice constant d is taken to be 25 \AA , molecules in outer shells would have to tunnel across a distance of $\sim 1 \text{ \AA}$. However, for $d = 25 \text{ \AA}$ and $\sigma = 3 \text{ \AA}$, we have $\Delta \approx -0.107 A$, consistently shifting the energy per particle of the 2D crystal to a lower value than the energy per particle inside the corresponding well (see Fig. 4.5), for any value of the well depth A . Thus, the condition of stability of the cluster crystal is not met, as the system finds energetically more favorable to form its equilibrium 2D crystal (leaving a fraction of the cell empty, as the density is below the equilibrium one). The breaking down of the

cluster crystal with the formation of the equilibrium 2D lattice was actually observed in simulation.

If the lattice constant d is taken to be nearly 30 Å (which would entail a rather large tunnelling distance across sites of approximately 6 Å), then $\Delta \sim -0.073 A$; in this case, the cluster crystal becomes energetically favored for $A \sim 100$ K, but the superfluidity of the cluster is suppressed in a such a deep well, as shown in Fig. 4.1. In order to make the cluster crystal energetically favorable, for a depth A such that the clusters are still superfluid, the lattice constant d must be taken as large as 36 Å, making the distance across which molecules would have to tunnel prohibitively large.

Increasing the width σ of the well does not lead to different physics, for a cluster of this many $p\text{-H}_2$ molecules, because the energy per molecule in the well is shifted downward by an amount roughly equivalent to that by which the magnitude of Δ is increased. Moreover, the disruptive effect of confinement on the superfluid response is greater for this value of σ , as a result of which the lattice constant needed to make the cluster crystal thermodynamically stable is again above 30 Å.

The energy balance is more favorable for smaller clusters, i.e., $N=10$, whose radius is approximately 8 Å. In this case, for $\sigma = 3$ Å, the cluster crystal with $d \sim 20$ Å, for which $\Delta \sim -0.168 A$, is energetically favored for $A \gtrsim 60$ K; it should be noted that clusters of these sizes remain superfluid even for such deep confining wells. Indeed, on taking $A \sim 100$ K the cluster crystal is favored over the equilibrium 2D crystal even for d as low as ~ 19 Å (because we are considering molecular tunnelling, a difference of 1 Å is significant). Tunnelling of molecules across adjacent clusters would involve in this case a distance of 3-4 Å. Whether that can allow for a superfluid phase at an attainable temperature

remains to be established. The main result of this study, however, is that a superfluid cluster crystal phase of $p\text{-H}_2$, if at all attainable, should have a number of molecules per unit cell equal to ten or less.

CONCLUSIONS

We have presented in this thesis, a low temperature systematic theoretical study of the properties of small parahydrogen clusters and the effect of confinement on the superfluid response and energetics, when trapped inside a Gaussian confining well. This was studied by means of Quantum Monte Carlo simulations achieved by using Worm Algorithm in the Continuous-space. The purpose was on the one hand to assess the robustness of the superfluid response predicted for the free clusters [20], on the other that of assessing the possibility of stabilizing a superfluid cluster crystal phase of p -H₂ in 2D, analogous to that observed in simulations for soft core bosons [14, 66].

The main physical conclusion is that 2D clusters retain in confinement most of the same physical properties of the free systems, at least within the range of confining parameters explored here. Clearly, the model of confinement adopted here is oversimplified; a more realistic physical model would presumably describe adsorption sites as impurities around which clusters would coalesce, i.e., with a short-distance repulsion between p -H₂ molecules and the impurity. This may have a suppressing effect on the superfluid response. Also, the effect of foreign substitutional impurities on the superfluidity of the clusters has not been addressed in this study. Based on the computed energetics, the stabilization of a superfluid cluster crystal phase seems possible if clusters are

relatively small ($\lesssim 10$ molecules), for a lattice constant some 20-25% greater than the characteristic size of the superfluid clusters. This would require p -H₂ molecules to tunnel across a distance of 3-4 Å, in order for phase coherence to be established across the whole system.

Bibliography

- [1] P. Kapitsa, *Nature* **74**, 141 (1938).
- [2] J. F. Allen and A. D. Misener, *Nature* **75**, 141 (1938).
- [3] F. London. *Phys. Rev.*, **54**, 947 (1938).
- [4] L. Tisza, *Nature* **141**, 913 (1938).
- [5] A. Griffin, D. W. Snoke, and S. Stringari. Bose-Einstein condensation. Cambridge, 1995.
- [6] M. Wolfke and W.H. Keesom, *Proc. Amsterdam* **31**, 81 (1927).
- [7] W. H. Keesom and G. E. MacWood. *Physica* **5**, 737 (1938).
- [8] *Phys. Rev. B.* **75**, 884 (1949).
- [9] C. E. Chase. *Phys. Rev.* **127**, 361 (1962).
- [10] J. G. Daunt and R. S. Smith. *Rev. Mod. Phys.* **26**, 172 (1954).
- [11] D. R. Tilley & J. Tilley, John Wiley & Sons Inc, New York, 1974.
- [12] R. M. Panoff and J. W. Clark *Phys. Rev. B*, **36**, 5527 (1987).
- [13] I. Beslic, L. Vranjes Markic, and J. Boronat, *Phys. Rev. B*, **80**, 134506 (2009).
- [14] S. Saccani, S. Moroni and M. Boninsegni, *Phys. Rev. B* **83**, 92506 (2011).
- [15] M. C. Gordillo and D. M. Ceperley. *Phys. Rev. B* **65**, 174527 (2002).
- [16] J. L. Tell and H. J. Maris. *Phys. Rev. B* **28**, 5122 (1983).
- [17] E. Molz, A. P. Y. Wong, M. H. W. Chan, and J. R. Beamish, *Phys. Rev. B* **48**, 5741 (1993).
- [18] M. Boninsegni, *J. Low Temp. Phys.* **168**, 137 (2011).

- [19] Germane to this idea is also the general notion that unusual bulk phases of matter can arise in properly designed confining environments. See, for instance, G. Stan, S. Gatica, M. Boninsegni, S. Curtarolo and M. W. Cole, *Am. J. of Phys.* **67**, 1170 (1999), and references therein.
- [20] S. Idowu and M. Boninsegni, *J. Chem. Phys.* **140**, 204310 (2014).
- [21] K. Yang, W. Xiao, L. Liu, X. Fei, H. Chen, S. Du and H.-J. Gao, *Nano Res.* **7**, 79 (2014).
- [22] T. Omiyinka and M. Boninsegni, *Phys. Rev. B* **90**, 064511 (2014).
- [23] M. Boninsegni, *Phys. Rev. A* **87**, 063604 (2013).
- [24] T. Dornheim, A. Filinov, and M. Bonitz, *Phys. Rev. B* **91**, 054503 (2015).
- [25] M. Boninsegni, N. V. Prokof'ev and B. V. Svistunov, *Phys. Rev. Lett.* **96**, 070601 (2006).
- [26] M. Boninsegni, N. V. Prokof'ev and B. V. Svistunov, *Phys. Rev. E* **74**, 036701 (2006).
- [27] D. M. Ceperley, *Rev. Mod. Phys.* **67**, 279 (1995).
- [28] See, for instance, D. M. Ceperley, in *Monte Carlo and Molecular Dynamics of Condensed Matter Systems*, edited by K. Binder and G. Ciccotti Editrice Compositori, Bologna, Italy, 1996.
- [29] R. P. Feynman. *Rev. Mod. Phys* **20**, 348 (1948).
- [30] D. M. Ceperley, *Rev. Mod. Phys.* **67**, 279 (1995).
- [31] M. Boninsegni, *Phys. Rev. B*, **79**, 174203 (2009).
- [32] S. Jang, S. Jang and G. A. Voth, *J. Chem. Phys.* **115**, 7832 (2001).
- [33] P. Sindzingre, M. L. Klein, and D. M. Ceperly, *Phys. Rev. Lett.* **63**, 1601 (1989).
- [34] L. D. Dang, *Superfluidity Near Localization : Supersolid And Super-glass:*, Doctoral Thesis, University of Alberta (2010).
- [35] See, for instance, F. Mezzacapo and M. Boninsegni, *Journal of Physics: Condensed Matter* **21**, 164205 (2009).
- [36] V. L. Ginzburg and A. A. Sobyenin, *JETP* **15**, 242 (1972).
- [37] M. Boninsegni, *Phys. Rev. B*, **70**, 193411 (2004).

- [38] M. Boninsegni, Phys. Rev. Lett. **111**, 235303 (2013).
- [39] M. C. Gordillo and D. M. Ceperley, Phys. Rev. Lett. **79**, 3010 (1997).
- [40] M. Boninsegni, New J. Phys. **7**, 78 (2005).
- [41] J. Turnbull and M. Boninsegni, Phys. Rev. B **78**, 144509 (2008).
- [42] K. Kuyanov-Prozument and A. F. Vilesov, Phys. Rev. Lett **101**, 205301 (2008).
- [43] P. Sindzingre, D. M. Ceperley and M. L. Klein, Phys. Rev. Lett. **67**, 1871 (1991).
- [44] F. Mezzacapo and M. Boninsegni, Phys. Rev. Lett. **97**, 045301 (2006).
- [45] F. Mezzacapo and M. Boninsegni, Phys. Rev. A **75**, 033201 (2007).
- [46] F. Mezzacapo and M. Boninsegni, J. Phys. Chem. A **115**, 6831 (2011).
- [47] A. Chizmeshya, M. W. Cole and E. Zaremba, J. Low Temp. Phys. **110**, 677 (1998).
- [48] F. Mezzacapo and M. Boninsegni, Phys. Rev. Lett. **100**, 145301 (2008).
- [49] I. F. Silvera and V. V. Goldman, J. Chem. Phys. **69**, 4209 (1978).
- [50] It is worth mentioning that refinements of the Silvera-Goldman pair potential have been recently proposed, affording a closer reproduction of the experimental equation of state of bulk p -H₂, especially under pressure. See, for instance, Refs. [51] and [52].
- [51] M. Moraldi, J. Low. Temp. Phys. **168**, 275 (2012).
- [52] T. Omiyinka and M. Boninsegni, Phys. Rev. B. **88**, 024112 (2013).
- [53] S. A. Chin, Phys. Lett. A **226**, 344 (1997).
- [54] J. E. Cuervo, P.-N. Roy and M. Boninsegni, J. Chem. Phys. **122**, 114504 (2005).
- [55] P. Sindzingre, M. L. Klein and D. M. Ceperley, Phys. Rev. Lett. **63**, 1601 (1989).
- [56] Y. Kwon, F. Paesani and K. B. Whaley, Phys. Rev. B **74**, 174522 (2006).

- [57] It is worth reminding that in a strict thermodynamic sense one cannot speak of “phase” of a finite system, hence the use of adjectives such as “solidlike” and “liquidlike”, which should be loosely interpreted in terms of qualitative, average properties of the system in its most probable configurations.
- [58] A. Sarsa, K. E. Schmidt and W. R. Magro, *J. Chem. Phys.* **113**, 1366 (2000).
- [59] M. Boninsegni and S. Moroni, *Phys. Rev. E* **86**, 056712 (2012).
- [60] C. Chakravarty, P. G. Debenedetti, and F. Stillinger, *J. Chem. Phys.* **126**, 204508 (2007).
- [61] J. E. Cuervo and P. N. Roy, *J. Chem. Phys.* **128**, 224509 (2008).
- [62] R. Guardiola and J. Navarro, *J. Chem. Phys.* **128**, 224509 (2008).
- [63] It should be mentioned that the calculation of the superfluid response at low T by means of the “area” estimator is rendered complicated for the more rigid clusters, by the occurrence of rigid rotations of the whole system (or, of one of several concentric rings) in the imaginary time interval $\hbar/k_B T$. Such rotations give rise to spurious, unphysically large values of the area estimator, from which there is no unambiguous way of extracting any genuine superfluid signal.
- [64] L. Dang, M. Boninsegni and L. Pollet, *Phys. Rev. B* **79**, 214529 (2009).
- [65] C. Cazorla and J. Boronat, *Phys. Rev. B* **88**, 224501 (2013).
- [66] See, for instance, M. Boninsegni, *J. Low Temp. Phys.* **168**, 137 (2012).
- [67] F. Cinti, P. Jain, M. Boninsegni, A. Micheli, P. Zoller and G. Pupillo, *Phys. Rev. Lett.* **105**, 135301 (2010).